Corrosion of tin and its alloys recovered from a 10th century wreck in the Java Sea

Ian D. MacLeod[1] & Mike Flecker[2]

[1] Department of Materials Conservation, Western Australian Museum, Cliff Street, Fremantle 6160
[2] Archaeological Salvage and Engineering, 132-B Grange Road, Singapore 249606

Abstract
A wide variety of corrosion products found on tin, bronze, lead and copper objects recovered from the *Intan* shipwreck in the Java Sea have been characterised. The nature of the wreck site is interpreted in terms of the changing burial environment of the objects over the past one thousand years. Comparisons of pewter corrosion products from cooler wreck sites in the Indian Ocean indicate that the "hot" equatorial waters have a major impact on the nature and extent of corrosion. The presence of both tin(II) and iron(III) corrosion products have been shown to exert a major influence on the nature of the crystalline calcareous deposits which form on tin-alloy objects.

Keywords
corrosion, tin-alloys, lead, copper, shipwrecks, temperature effects, seawater

Introduction

The *Intan* wreck lies in open equatorial waters of the north-western Java Sea, Indonesia, in position 4° 24' S and 106° 41' E. It is likely that a storm caused the loss of the vessel since the nearest navigation hazard is more than 60 km away. The wreck takes its name from the nearby Intan Oil Field, some 16 kilometres to the south and was archaeologically excavated in 1997. Chinese coins, stylistic analysis of ceramics, radiocarbon dating of ships' timbers and organic artefacts date to the period 918 to 960 AD. The ship was most probably sailing from a Srivijayan entrepot port, perhaps Palembang in south Sumatra, to a port in Java. The wreck lies on a plateau at a depth of 26 metres, with the seabed characteristics unchanged within a twenty kilometre radius of the site. The seabed is completely bereft of rock or coral outcrops with the only macro-benthic organisms being tube worms, gobies and a variety of shells. A layer of silty-sand, from 0.1 to 1.0 metre thickness, overlies stiff clay whose profile of up to 1 metre above the seabed is due to an earlier erosion regime which has left the clay surface holed and pitted. In several places there was a distinct intermediate layer of well consolidated silt, within which the artefacts were found. The top layer consists of a medium grained brown sand and shell grit with a little silt whilst the mid layer consists of a well consolidated silt mixed with fine sand. There was a 50 metre spread of artefacts and a low mound height of less than a metre. The extent of the site was delineated by the surface scatter of ceramics, mostly shards, along with some iron concretions but all other metal artefacts were buried.

The site is subject to the typical southern hemisphere tropical monsoon pattern which sees the south-east monsoon run from May to September and the north-west monsoon from November to March. There is a transition period of variable winds and calms between monsoons. With the relatively short fetches in the Java Sea, strong monsoon winds can lead to steep, short crested waves and swells of only two metres could be felt by the divers 26 metres below on the seabed. The *Intan* site is subjected to variable currents resulting from the combined influence of monsoon currents, tidal movement and local meteorological conditions. When all factors combine, the current can reach two knots but during excavation activities the currents rarely exceeded one knot or 0.54 m / sec. Marine atlases indicate that the mean annual water temperature is 29±0.8°C [1] and the actual recorded temperatures varied from 28°–29°C Like most wrecksites in an apparently sterile environment, the site was extremely well stocked with fish, but corals and sponges were scarce. A few soft whip corals and sponges of varying colour decorated some shards. Others were encrusted with small oyster shells and tube worm casings but there were almost no encrusting corals. This is in stark contrast to the nearby 13th century *Java Sea* site [2] which indicates that the *Intan* site has been buried for a significant period. The anti-fouling properties of copper and tin corrosion products may also have played some role in this phenomenon since approximately two tonnes of

dome-shaped bronze ingots were found on the site. Only a few fragments of wood of the original ship remained while metal artefacts, tin, silver and bronze ingots all remained in the vicinity of the original wreck position.

The general distribution of artefacts is consistent with the massive and concentrated weight of the metal cargo keeping the site inherently intact for a prolonged period while marine borers ate away the timbers and currents eroded the surrounding seabed. Subsequently ceramic materials migrated down the mound and so formed the nature of the present site. More recent increased river runoff has seen increased sedimentation on the site where it now has an average thickness of 0.3 metres. Although the site is 26 metres deep, major storms do stir up the sediment in the top layers, and impart momentum to the exposed artefacts. While the wrecking process had reached a very advanced level, it was still ongoing right up to the time of the excavation.

Analysis of corrosion products

Corrosion products from both shipwrecks were examined by optical microscopy and automated powder diffraction (XRD) and SEM-EDXRA analysis to determine the nature of the degradation processes. Phases of corrosion products were also identified by Debye-Scherrer X-ray patterns. Reference numbers quoted after object identification relate to analytical reports from the Materials Institute of WA (MIWARP). Macrophotographs were taken using an Olympus Stereo-Microscope and Nikon Macro-System. Quantitative elemental analysis was carried out using inductively coupled plasma – atomic emission spectroscopy (ICP-AES) after digestion with concentrated sulphuric acid. Quantitative analytical results are reported in either parts per million (ppm) or as weight percent unless otherwise noted. Some phases were also investigated using Fourier transform infrared spectrometry (FTIR).

Corrosion products on the *Intan* wreck

Amongst the variety of materials recovered from the wreck were a series of **plano-convex bronze ingots** (210-6), approximately 9 cm diameter and a maximum thickness of 2 cm, was mainly composed of 93% copper and 6%wt tin and 1%wt lead. The surface of the ingot was rough and pitted especially on the planar side. The seawater had deposited white aragonite, orthorhombic $CaCO_3$, light brown Sn(IV) minerals schoenfliesite [$MgSn(OH)_6$], brown cassiterite [SnO_2], brassy chalcocite Cu_2S, black djurelite $Cu_{31}S_{16}$, black tenorite [CuO], quartz [SiO_2] and green copper chloride hydrate [$Cu_2(OH)_3ClH_2O$]. The SEM data indicated that the corrosion matrix reflected the underlying composition of the bronze alloy in that lead was only present in trace amounts. There was a trace amount of phosphorus in a blue matrix that was dominated by copper but also had minor amounts of calcium, sulphur, tin and magnesium. SEM analysis of the polished cross-section of the ingot showed up significant gas porosity associated with the casting process, the porosity near the surface enhanced localised corrosion and lead to the development of cavities, which were rich in cuprite. In the dendritic structure, the α phase consisted of a solid solution of 3% Sn and 0.5% Pb in 96.5% copper and the (α+δ) phase consisted of 71% Cu, 27% Sn and 2% Pb, as shown in Figure 1. The lead in the ingot tended to be distributed close to the boundaries between the primary α and the dendritic α+δ phase, with the composition of 88% Pb, 11% Cu and 1% tin, as seen in Figure 2. The presence of

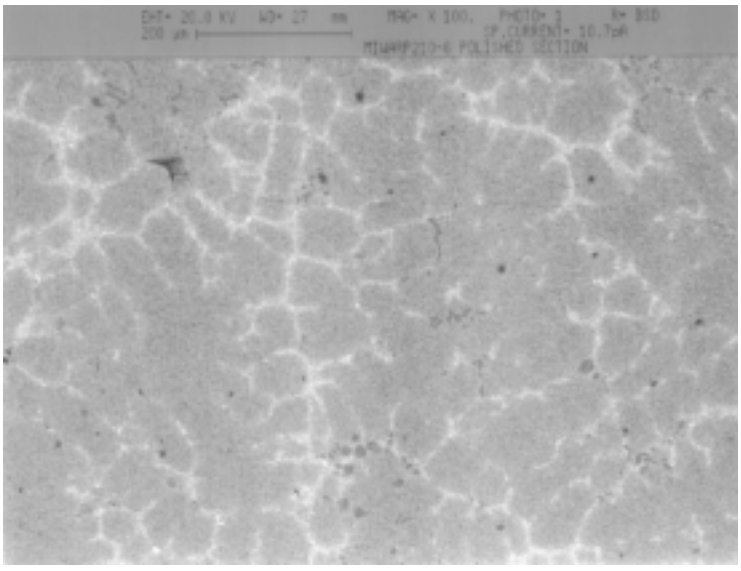

Figure 1. Backscattered SEM image (x 100) of the polished plano-convex copper ingot 210-6 showing dendritic phase 2 (27% Sn, 71% Cu, 2% Pb) in a dark phase ground mass (3% Sn, 96.5% Cu, 0.5% Pb). Most of the bright phase 3 (1%Sn, 11% Cu 88% Pb) was confined to phase 2. The very dark rounded spots were a copper sulphide.

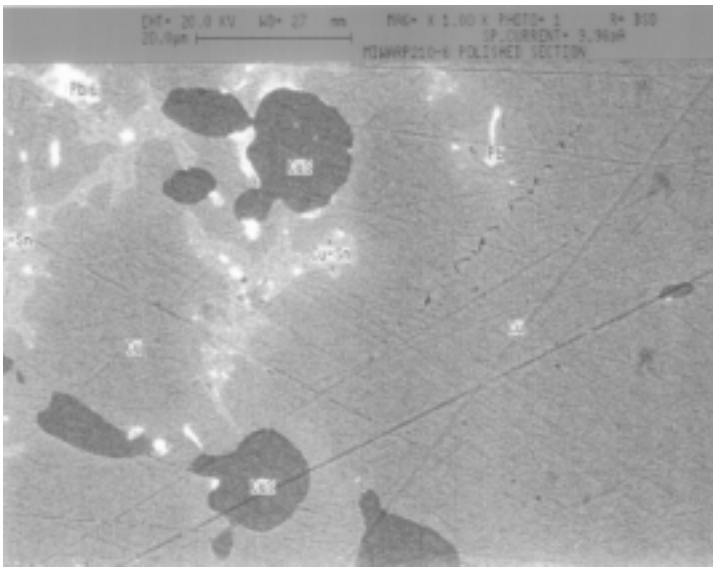

Figure 2. Backscattered SEM image (x 1000) detail of 210-6, showing the dendritic light phase 2 marked ***Cu-Sn*** (27% Sn, 71% Cu, 2% Pb) in a dark ground mass phase 1 marked as ***Cu*** (3% Sn, 96.5% Cu, 0.5% Pb). Most of the bright phase 3 marked as ***Pb*** (1% Sn, 11% Cu 88% Pb) was confined to the interdendritic phase 2 marked as ***Cu-Sn***. The very dark rounded spots were a copper sulphide.

both aerobic and anaerobic corrosion products on the bronze ingots is proof of the varying degree of aeration on the wreck site. The presence of tenorite is unusual as it had previously only been reported from the interior of the composite gun from the wreck of the *Batavia* (1629) in the Abrolhos Islands off the Western Australian coast, some 450 km north of Perth. It is believed that the tenorite had been formed as a result of the copper bore of the gun becoming heated during live firing [3]. The presence of the sulphides djurelite and chalcocite is clear evidence that the site has been subjected to significant periods of burial.

Apart from the small **bronze ingots** there were a number of worked bronze artefacts, which included a bronze mirror (210-7), approximately 4mm thick, composed of 71.20±0.60% copper, 25.2±0.20% tin and 3.50±0.90% lead. Despite the presence of adventitious iron corrosion products, the non-ferrous corrosion deposit on the surface of the sample was mainly composed of poorly crystalline cassiterite [SnO_2] and cuprite [Cu_2O] with a minor amount of an unidentified calcium carbonate. Minor spots of an unidentified copper sulphide were also detected. The SEM data indicated that phosphorus was also present as a trace element in the cassiterite matrix and that whilst no specific lead corrosion products were characterised, this metal was reporting at the minor component level, which is consistent with the four-fold increase in concentration in the parent alloy, compared with the bronze ingot. Trace amounts of aluminium and potassium were periodically found in the corrosion product matrices but this is just a reflection of their adventitious presence in clay minerals. A polished section of the mirror showed up inclusions of copper sulphides, with some iron, which came from the parent minerals used in the manufacture of the mirror. It is likely that the original minerals may have included the copper-iron sulphide chalcopyrite, $CuFeS_2$ as well as chalcocite Cu_2S.

The analysis of the metal phases revealed in the sectioned object showed it was typical of Chinese **bronze mirrors** [4]. The backscattered SEM showed up the as-cast cored dendritic microstructure with the copper rich phase having 11% more copper than the mean composition at 82.00±1.10% copper, 16.7±0.70% tin, and 1.20±0.50% lead. The bulk of the dendritic structure showed no statistically different composition for tin and copper, compared with the overall values, but the lead content was significantly lower at 2.10%. This is simply a reflection of the fact that most of the lead in the alloy was distributed as micodroplets, approximate diameter 5mm, and these droplets analysed at 90.4±0.9% Pb, 7.9±0.7% Cu and 1.6±0.2% tin. The segregation of the alloying elements in the phases of the mirror is reflected in the ratios of tin to copper, which had a mean value of 0.35 for the bulk of the metal and the tin-rich inter-dendritic phase, but the ratio fell to 0.20 in the copper-rich phase and in the lead droplets [5]. The similar values of tin to copper in the α phase and the lead droplets indicates that the ultimate distribution of the alloying elements is determined by their primary activity in the copper-rich α phase.

Attached to the **bronze mirror** was a mass of crystals which were composed mainly of aragonite, magnesium calcite [$(Ca,Mg)C0_3$], calcite [rhombohedral $CaCO_3$] and gypsum $CaSO_4.2H_20$. The gypsum occurred as brown crystals attached to the top of the convex side of the artefact. The

white friable deposit on the surface of the convex side of the artefact was composed of aragonite, calcite and amorphous silica. The hard grey crust beneath this layer was composed of aragonite and magnesium calcite. The concave surface of the artefact was composed mainly of mollusc remains. This form of calcareous deposit has not been previously reported on bronze objects recovered from historic shipwrecks. Since the solubility of calcium carbonate is inversely proportional to temperature, the accumulation of calcareous materials on top of the mirror may be due to a combination of the relatively high seawater temperatures and the cathodic reduction of dissolved oxygen providing a localised increase in pH, which leads to the selective precipitation of the magnesian calcites. Similarly, massive calcite crystals have been identified on objects recovered from the Pattaya wreck in the Gulf of Thailand [6]. The SEM analysis of the calcareous matrix showed up the presence of chloride as a major component but no specific chloride-containing phases were identified by x-ray diffraction.

Given that calcium carbonate is essentially saturated or supersaturated in normal seawater, the processes controlling crystallisation will tend to have a disproportionate effect on the inorganic concretion formation. The presence of magnesium brings about a marked change in the kinetics of precipitation of calcite since "the power of dependence of the rate of nucleation increases from a second to a six order in the presence of magnesium"[7]. Normally calcium will precipitate as $CaCO_3$ in preference to gypsum. It is generally acknowledged that aragonite is thermally unstable with respect to calcite but gypsum seems to have a marked stabilising effect on the rate of conversion of aragonite to calcite [8]. Several authors believe that the precise form of carbonate precipitate is kinetically controlled by the degree of super saturation [9]. The primary trace elements, which have a major effect on the mineralogy of calcite and aragonite, are those whose size and charge make them suitable substitutes for calcium and magnesium. The most important ion in this study is Sn^{2+} since it's radius is 0.93Å while calcium is 0.99Å [10]. Thus the presence of localised concentrations of tin(II) is going to be seen as a localised increase in the ionic product of calcium and this can initiate crystallisation. The ionic radius of the Fe^{3+} ion is 0.64 Å and Mg^{2+} is 0.66 Å and so the presence of adventitious iron(III) corrosion products may well have a major influence on mineralisation phenomena. The rates of conversion of aragonite to calcite are a very significant geological process and at seawater temperatures encountered and with the age of the wreck, the conversion rate of 10 mm/year at 25°C becomes significant after 1000 years [11].

Amongst the artefacts recovered from the site was a **pewter rod** (210-3) measuring 6.5 cm length and l.25 cm in width. At each end and in the middle of the fitting, there were protrusions, which were clasps for clamping the rod, which was a form of currency, onto a string (see Figure 3). The overall composition consisted of 54.2±0.7% wt tin and 45.8±0.6% wt lead. Since the bulk composition is similar to the eutectic composition of 61.9% Sn for the tin-lead phase diagram, the microstructure will naturally mainly consist of a tin-rich and a lead-rich phase of the eutectic mixture [12]. The backscattered SEM images clearly demonstrate that the lead rich phase, 94% Pb and 6% Sn, has been selectively attacked, compared with the tin-rich, 97% Sn and 3% Pb, phase. The corrosion deposits on the surface of the fitting were mainly composed of cotunnite [$PbCl_2$], laurionite [PbCl(OH)] and cerussite [$PbCO_3$] with some plattnerite [PbO_2] and possibly a tin oxide. Traces of iron, at 0.2±0.1%, were detected in the lead-rich phase, which consisted of 93.5% lead and 6.3% tin. This may be a reflection of iron contamination from a mould that was used in the manufacture of the object. The morphology of the corroded surface, which showed selective attack on the lead-rich phase, is reflected in the domination of the corrosion products by lead species. As with the case of the bronze ingots, there were varying amounts of phosphorus, from minor to trace levels, in the corrosion matrixes along with aluminium and potassium from the clay deposits on the seabed. The presence of plattnerite as one of the major lead corrosion products was unexpected, since oxidation

Figure 3. A macrophotograph of the pewter rod 210-3 showing the white deposits of cotunnite [$PbCl_2$], laurionite [PbClOH], cerussite [$PbCO_3$] and traces of dark plattnerite [PbO_2]

products containing the oxide moiety have been previously associated only with high energy sites, in the subtropical waters off the Western Australian coast [13]. It is likely that the cause for the difference in the corrosion products lies in the different temperatures of the *Intan* site which is at least 5°–7°C since the presence of laurionite, cotunnite and cerussite are all commonly found on turbulent shallow water sites [14].

One of the **pewter corrosion pustules** (118-4) was broken on recovery and the interior matrix consisted of a dark grey soft waxy, non-crystalline inner core with a beige crust composed of cassiterite SnO_2. The waxy material, examined by Fourier Transform Infrared (FTIR) spectroscopy, exhibited a shoulder absorbance at 3378.4 cm^{-1}, a very broad absorption with a peak at 1229.6 cm^{-1} and metal oxygen and metal chloride stretching peaks at 625.5 cm^{-1} and at 517.4 cm^{-1} respectively. The broad absorption envelope from 800–3500 cm^{-1} is characteristic of a number of amorphous phases being present, as there are several humps within the envelope, which are consistent with materials of poorly defined crystalinity (Figure 4). The contents of the blister were also examined using the thin-window mode of operation of the SEM, which allows for identification of light elements such as oxygen. All the phases in the waxy material had tin as their major element and varying proportions of chlorine, oxygen, silicon and copper as trace components. All the evidence indicates that the matrix consists of a mixture of an amorphous tin hydroxy chloride, possibly incorporating some solubilised silica from the sediment, since no discrete silicon phases, such as SiO_2, could be identified by XRD.

Detailed examination of the surface crust of the blister showed that it contained massive grey cassiterite fragments with a light brown surface deposit composed of cassiterite with a trace of tin chloride [$SnCl_2$] similar to JCPDS pattern no. 18-1265. The light brown phase on the surface had the similar abundance of the same elements as the bulk grey phase i.e. oxygen, chlorine and silicon. The underlying metal rod was sectioned which showed that the round ingot had a core of platy abhurite [$Sn_3OCl_2(OH)_2$] with a minor unidentified poorly crystalline phase (probably also a tin chloride hydrate) with a dark rim mainly composed of romarchite [SnO] and a minor unidentified tin oxide, with a trace of a probable tin chloride hydrate. Also present were yellow crystals (probably a tin chloride hydrate) associated with the platy abhurite in the core of the ingot and a minor unidentified phase. The surface of the ingot had a trace of light brown cassiterite and an iron-rich clay material with indicative elements of silicon, aluminium, oxygen supporting the identity of an iron alumino-silicate. A further section of the round ingot showed a dense platy abhurite core surrounded by an intricate matrix of dark romarchite with a minor unidentified tin phase and light brown patches composed of abhurite, romarchite, cassiterite and tin. There were

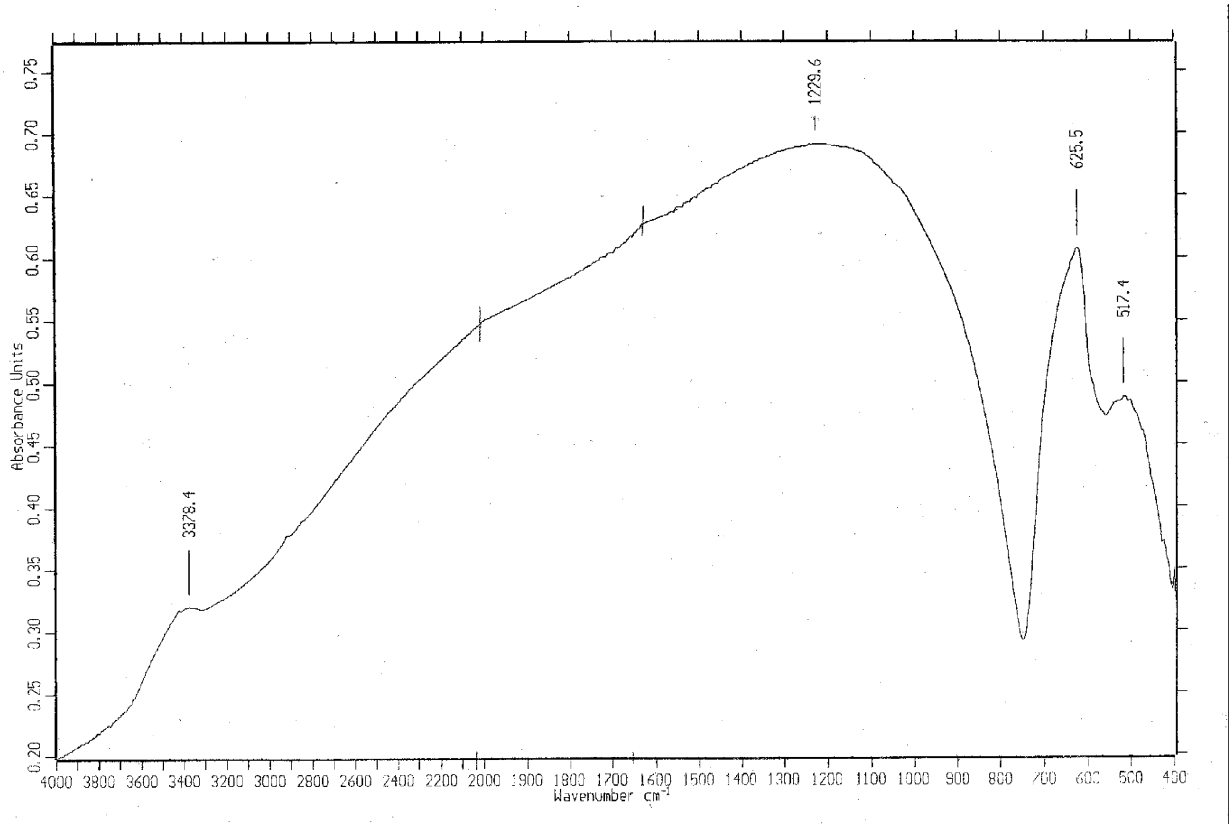

Figure 4. An FTIR spectrum of the amorphous tin corrosion products found inside a pustule on sample no 118-4.

unidentified phases (probably tin oxides) associated with the black romarchite and lighter brown cassiterite patches. There were minor phases of tin chloride hydrates and tin oxides associated with the ground mass and black romarchite which could not be positively identified. It is likely that the presence trace amounts of magnesium reflects small amounts of minerals such as schoenfliesite, $SnMg(OH)_6$ and that the iron is adventitiously present in the corrosion matrix.

The **plano-convex pewter ingot** (210-5) had a circumference of 4.5cm and a thickness of 1.5 cm and was composed of 72.5%wt tin and 27.5%wt lead. Like the pewter ingot described above, the common corrosion deposits were cerussite [$PbCO_3$], laurionite [PbCl(OH)] with a minor amount of plattnerite [PbO_2]. The only significant difference is that the pewter ingot also had cassiterite [SnO_2] on the surface. The SEM analysis showed that the white bulk corrosion products were dominated by tin, with trace amounts of lead, chloride, copper and silicon and that the light brown materials on the surface mainly consisted of calcium (carbonates) with entrapment of tin and lead corrosion products, along with clay minerals (see Figure 5). The quantitative analysis of the polished sectioned metal is shown below in Table I.

It is likely that the presence of cassiterite as a corrosion product on the surface of the ingot is due to the extra amount of tin in the alloy, compared with the pewter rod, since this ingot is hyper-eutectoid whilst the latter was hypo-eutectoid. The analysis of the different phases in the metal clearly demonstrates that the tin-rich phase is essentially pure tin and that the lead-rich phase has a moderate amount of tin dissolved in it in a solid solution. From the domination of the corrosion products by lead, it is clear that the shipwreck environment favour selective corrosion of the lead-rich phases of the pewter.

One pewter object consisted of a thin section of metal, which was totally concreted with a calcareous matrix and was essentially fully mineralised. It principally consisted of cassiterite and romarchite, which occurred as dark spots and also as a thin dark crust. Abhurite was only detected in a small area of the specimen. Some areas of the cassiterite were stained blue from copper corrosion products.

A **round tin ingot** (118-1) was partly covered with a layer of abhurite [$Sn_3OCl_2(OH)_2$] and cassiterite [SnO_2] and the SEM analysis showed that the underlying platy fragments had tin and chlorine as major components and that silicon and oxygen were minor elements. A small sample of the underlying metal was dissolved and the analysis, Table II, showed up a remarkably pure tin, with only low levels of lead impurities and trace amounts of copper and zinc in the metal. The selective corrosion

Table I: SEM quantitative analysis of the hyper eutectoid plano-convex pewter ingot.

Bulk phase x 100	Sn	Pb	Fe	Sn/Pb Ratio
Mean bulk composition	72.5 ± 0.6	27.4 ± 0.6	<0.1	2.64
BSD[1] Bright spot x 300 lead-rich phase	4.4 ± 1.1	95.6	<0.1	0.05
BSD Dark spot x 300 tin-rich phase	99.4 ± 0.3	0.5 ± 0.3	0.1	198.8
Mean image phase analysis x 100	75.6 ± 1.9	24.4 ± 1.9		3.09

[1] BSD is Back Scattered Detector mode of SEM operation

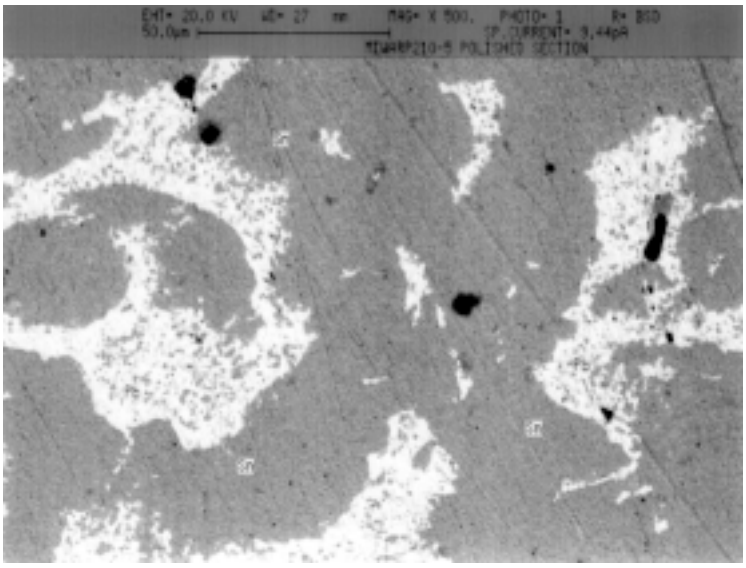

Figure 5. SEM of detail structure on the plano-convex pewter ingot 210-5. The backscattered showing the dark tin-rich phase of 99.5% Sn and 0.5% Pb and the light lead-rich phase containing 4.5% Sn and 95.5% Pb. Magnification X 500

Table II: Analysis of a tin ingot from the *Intan* shipwreck

Sample	Sn %	Sb ppm	Zn ppm	Pb ppm	Si ppm	Cu ppm
Round ingot metal – lot 1	99.60	**nd**	**10**	**190**	**nd**	**8**
Round ingot metal – lot 2	98.40	**nd**	**60**	**1750**	**nd**	**18**
Surface corrosion products	37.90	**70**	**250**	**850**	**980**	**94**

of zinc, copper and antimony from the underlying metal is typical of the localised corrosion around the primary ± tin phase. The thin window mode analysis of the corrosion products showed up trace amounts of copper and zinc, along with oxygen and chlorine, which supports the general observation of the sensitivity of this mode of analysis, since traditional operational modes would not have detected the trace levels of copper and zinc.

The corrosion products on a second **oblong tin ingot** (210-2), which measured 3.3 x 4.8 cm, with a convex lens up to a maximum of 7 mm thickness, was dominated by cassiterite, romarchite [SnO] and abhurite. The sample had a 1 mm thick crust of romarchite and cassiterite overlying a blister that had fine needles of cassiterite overlying platy abhurite crystals and residual metallic tin (see Figure 6.) The blister is typical of the morphology associated with the internal pitting corrosion of tin alloys, since the internal pressure of the increased volume of corrosion products results in the plastic deformation of the parent alloy. The cross-section of the blister showed up residual microstructure of the original surface. The absence of lead corrosion products is consistent with the analysis of the ingot, which was 99.7±1.7 % tin and 0.4±0.3% iron. Abhurite and tin (II) chloride were also found during corrosion simulation experiments on the corrosion of tin alloys in natural seawater, especially in simulated crevices [15].

Analysis of some silver and lead objects from the *Intan* wreck also provide evidence of the overall chemical environment of the wreck site. A silver ingot was composed of 95 % Ag, 3.5 % copper and a very high gold content of 1.5% and was covered with a layer of acanthite, Ag_2S and the SEM analysis showed up copper and gold as minor components on the surface of the corroded ingot. This clearly shows that the environment was anaerobic for some significant period of time, most likely associated with burial under some of the clay minerals. A small pewter ingot had also corroded in an anaerobic environment since it was covered with galena [PbS] that was overgrown with cotunnite [$PbCl_2$], along with traces of laurionite [PbCl(OH)] and a tin chloride hydrate [$SnCl_2.2H_2O$]. The secondary aerobic corrosion products growing on top of the galena is a clear indication that a major site

Figure 6. Microphotograph of a cross-section of the 210-2 oblong tin ingot corrosion pustule showing surface deposits of calcium carbonate and quartz. A layered crust is also seen (0.1 cm thick) which contains a darker layer of romarchite and a lighter layer of cassiterite. The core was composed mainly of relic metallic tin and interstitial abhurite. Approximate magnification x 11.

disturbance had taken place and changed the anaerobic microenvironment to one that was clearly aerobic which corroded out both tin and lead from the parent metal matrix. Another sample of buckled and bent lead sheet had totally mineralised and was composed of hydrocerussite [$Pb_3(CO_3)_2(OH)_2$] and black plattnerite [PbO_2] but it had a clearly banded or layered collection of corrosion products which indicated that the site has had prolonged periods of different levels of exposure.

Discussion

In order to properly review the decay of the tin alloys on the *Intan* wreck, it is useful to summarise the occurrence of all the various corrosion products, which have been found on the site, as shown in Table III. It has been previously noted that tenorite, CuO, has only been found on one wreck site off the Western Australian coast and that the artefact itself had been subject to localised heating during gun firing. Previous studies [13] had reported that lead corrosion products containing the oxide ion, such as plattnerite PbO_2 and litharge PbO, were generally associated with the highest energy sites where a combination of shallow waters and reefs lead to very turbulent conditions and high degrees of oxygenation. Clearly the presence of plattnerite on the *Intan* site cannot be the result of turbulent water flow, nor can the presence of chloride rich corrosion products such as cotunnite $PbCl_2$ be due to the same phenomena. The most likely cause for the difference in behaviour must lie in the higher average water temperatures is sufficient to overcome the activation energies associated with the various rate-determining steps in the overall corrosion process. In order to gain a clearer understanding of the significance of the data on corrosion products from the *Intan* wreck, it is constructive to review corrosion processes on pewter objects from shipwrecks in cooler waters.

The wreck of the Dutch Eastindiaman *Zuytdorp* which sank at the foot of the eponymous cliffs in 1712, providing a wreck site with a characteristic high energy zone, in which bronze cannon have been eroded to less than 10% of their original dimenstions by the relentless pounding of the surf. Apart from the differences in turbulence between the Java Sea and this Indian Ocean site, the *Zuytdorp* site has mean water temperatures of 22.2°±1.9°C which is significantly cooler than the *Intan* site at 29.0±0.6°C [1]. The wreck of the American China Trader *Rapid* is located approximately 600 km north of the *Zuytdorp* and the mean temperature of that site is 24.0±1.6°C and there are corresponding differences in the way in which tin and lead corrosion products are formed on pewter objects. The *Zuytdorp* pewter objects comprised a set of four bottle tops, some of which still retained the original glass. For both ZT 3358 & 3359 the inside and the outer rims were mainly covered with areas of aragonite [orthorhombic $CaCO_3$] and quartz [SiO_2] with some red magnetic iron oxides, however the top of the outer part of the cap was encrusted with clear crystals of calcite [rhombohedral $CaCO_3$] and magnetic iron oxide, along with fine white cerussite [$PbCO_3$]crystals.

A fragment of ZT 3359 showed that the pewter is metallurgically comlex as there were four different phases; a primary tin-rich phase (97% Sn and 2% Pb), a lead-rich phase (3.8% Sn and 86.8% Pb), a minor tin-copper phase (not analysed) and a "tin edge" around the pewter (96% Sn and 1% lead). The overall composition was 62.90 ± 1.00 wt% tin and 36.55 ± 1.40 wt % lead with an average amount of 0.38 wt % copper which is essentially the eutectic composition of Sn_3Pb. Thus the pewter bottle tops would have solidified close to the eutectic temperature of only 183°C and that the outer tin-rich zone is probably due to a form of "tin-sweat" where the low melting point of the tin resulted in it mobilising to the edge of the mould [12]. This pewter top had a thin crust of romarchite [SnO] and an inner thicker layer of cotunnite [$PbCl_2$] underneath the calcareous deposit (see Figure 2). Analysis of the other sections of the corroded metal showed that there were zones where the tin had essentially been totally mobilised, leaving the partly corroded original lead-rich phase of the eutectoid. Within this matrix the sulphur content varied between zero and a maximum of 2.4% which is strongly supportive of some lead sulphate or other corrosion products also being present, as the total value of materials was only 91.82 ± 2.56 %. Given the ability of iron(III) corrosion products to concentrate sulphate ions [14], it is likely that the adventitious iron corrosion products on the outer parts of the bottle tops would have increased the localised concentration of sulphate to allow some products to precipitate. An outer section of the pewter cap exhibited the mirror image of the selective corrosion in which nearly all the lead had corroded away to leave 97.1% tin and 2.1% lead.

The presence of romarchite, SnO, on the inner surfaces of the bottle cap ZT3360 is an indication that the object had settled topside-up and that the lower level of oxygen has lead to selective corrosion and precipitation of tin(II) on the inner surfaces. There was also some romarchite mixed in with the calcareous deposits on the seaward surface of the bottle top. Some of the surface contained magnesian calcite, the precipiation of which may well have been facilitated by the presence of Fe^{3+} [7]. A fourth pewter bottle cap ZT 3361 had some aragonite on the outer top surface, although calcite was present it was less abundant than in the other three samples. The presence of the sand grains is an indication of the temporary burial of the object. This data supports the supposition that different corrosion processes took place according to the seasonal changes when large sections of the site are covered

Table III: Corrosion products found on the 10th century *Intan* wreck

Compound	Formula	Objects
Abhurite	$Sn_3OCl_2(OH)_2$	Tin ingot: 118-1, Pewter rod: 118-5, Round ingot: 118-6A, Tin ingot 210-2, Pewter 210-4,
Acanthite	Ag_2S	Silver billet: 210-1
Aragonite	$CaCO_3$, orthorhombic	Pewter rod: 118-5, Bronze ingot: 210-6, Bronze mirror: 210-7, Bronze mirror: 210-9
Calcite	$CaCO_3$, rhombohedral	Bronze ingot 210-6, Bronze mirror: 210-9
Cassiterite	SnO_2	Tin ingot: 118-1, Pewter rod ingot: 118-3, Bronze object: 118-4, Pewter blister: 118-5, Round ingot: 118-6A,B, Tin ingot 210-2, Pewter 210-4, Pewter ingot: 210-5, Bronze ingot: 210-6, Bronze mirror: 210-7
Cerussite	$PbCO_3$	Pewter 210-3, Pewter ingot: 210-5, Bronze mirror: 210-9
Chalcocite	Cu_2S	Bronze ingot: 210-6
Cotunnite	$PbCl_2$	Pewter 210-3, Bronze mirror: 210-9, Pewter rod 210-11,
Copper hydroxy chloride	$Cu_2(OH)_3Cl$	Bronze ingot: 210-6
Cuprite	Cu_2O	Bronze mirror: 210-7
Djurelite	$Cu_{31}S_{16}$	Bronze ingot: 210-6
Galena	PbS	Lead ingot 210-11
Gypsum	$CaSO_4.2H_2O$	Bronze mirror: 210-9
Hydrocerussite	$[Pb_3(CO_3)_2(OH)_2]$	Pewter blister: 210-8
Laurionite	PbCl(OH)	Pewter 210-3, Pewter ingot: 210-5, Bronze mirror: 210-9, Pewter rod 210-11
Magnesian calcite	$(Ca,Mg)CO_3$	Bronze mirror: 210-9
Plattnerite	PbO_2	Pewter 210-3, Pewter ingot: 210-5, Pewter 210-8, Bronze mirror: 210-9,
Romarchite	SnO	Pewter rod ingot: 118-3, Pewter rod: 118-5 Round ingot: 118-6A,B, Tin ingot 210-2 Pewter 210-4
Schoenfliesite	$MgSn(OH)_6$	Bronze ingot: 210-6
Tenorite	CuO	Bronze ingot: 210-6
Tin chloride	$SnCl_2$	Pewter rod: 118-5
Tin chloride hydrate	$SnCl_2.2H_2O$	Pewter rod 210-11

in sand. Subsequent storms expose the site to the full brunt of the surge. Studies on the corrosion behaviour of bronzes in seawater subjected to different levels of aeration show that thermodynamically favoured corrosion of tin occurs under conditions of low oxygen availability [16,17]. The data indicates that there is selective corrosion of the lead-rich phases in the fully exposed condition and corrosion of the tin-rich materials in the time of poor oxygenation or burial. Potentiodynamic scans of tin in pH environments similar to seawater has shown that the oxidation process clearly goes via a two-step process with Sn(II) corrosion products resulting from the primary oxidation step [18]. Other work involving corrosion measurements in varying chloride and dissolved oxygen concentrations showed that the actual rate of corrosion of tin can be higher under a nitrogen atmosphere [19]. These studies on pure tin electrodes help to explain the varying selective corrosion processes which have taken place on the *Zuytdorp* site and they also clarify the passivating role of the primary layer of romarchite, which clearly exerts some inhibitory effect.

None of the pewter bottle caps showed any significant signs of colonisation by sedentary epifauna and this is probably a reflection of the toxicity of the tin corrosion products which were continuously being produced and dispersed by the strong water currents of the surf zone. If we compare the virtual absence of tin corrosion products from the surfaces of these eutectoid pewters to the large amount of chloride-containing and Sn(II) hydroxy species on the *Intan* pewters (see Table IV), the reason may well lie with the turbulence of the *Zuytdorp* site, which normally does not permit a sufficiently high concentration of tin(II) to accumulate to allow for precipitation. Given that the mean temperatures of the *Intan* and *Zuytdorp* sites differs by more than 5°C, the decreases in oxygen solubility amounts to a drop of 10% in the maximum amount of dissolved oxygen that is available on the *Intan* site [20]. The difference in dissolved oxygen concentrations may be a contributing factor to the number of divalent tin corrosion products on the *Intan* site. That turbulence is the most likely cause for the different behaviour of the pewters on the two sites is further supported

by analysis of some pewter buttons from the wreck of the *Rapid* (1811), listed as RP3884, which lies in relatively sheletered waters at a depth of seven metres and in warmer waters than the *Zuytdorp*. Both schoenfliesite [$Sn_3OCl_2(OH)_2$], a tin hydroxy chloride $Sn_{21}Cl_{16}(OH)_{14}O_6$ and the other Sn^{2+}corrosion product $Sn_4(OH)_6Cl_2$ were all found on the surfaces of the pitted buttons, which had bulk composition of 86.5% Sn, 7.6% Pb and 7.3% copper. Given that the buttons were clearly a hyper-eutectoid composition, the dominance of tin in the corrosion products is not unexpected.

Conclusion

The mineralisation of tin and its alloys with copper and lead have been shown to be very sensitive to the composition of the alloy and to the associated microstructure. Under the turbulent conditions of the *Zuytdorp* there is a paucity of tin corrosion products on the surface of pewters owing to the loss of tin into solution during the combined processes of oxidative hydrolysis. When the object is protected from the gross wave action, the normal range of tin(II) corrosion products are dominated by romarchite [SnO] and are found on the interior of the object or in lenses created by pitting corrosion pustules. The preferential deposition of calcite on the outer surface of the pewters is believed to be due to the combintion of surface concentrations of tin(II) ions, which mimic Ca^{2+} ions in terms of their size and inherent ionic strength and the precipitation of adventitious iron(III) corrosion products which create local increases in the sulphate concentration. Thus the net ionic product for calcium ions and carbonate ions is increased to the point where calcite crystallises from seawater. By applying the same reasoning to the *Intan* site, we can see that the most probable cause of the massive growth of calcareous materials on the bronze mirror was the high surface concentrations of Sn^{2+} ions which mimicked Ca^{2+} ions and so lead the the crystallisation of all the calcareous minerals. It is most likely that this process took place when the mirror was partly buried under the sediment and there was selective attack on the tin-rich phases of the bronze. The absence of sulphide corrosion products on the mirror shows that it was not put under anaerobic conditions for any length of time, for otherwise anaerobic corrosion products would have formed.

A further factor controlling the precipitation of calcium carbonates and sulphates on the *Intan* site is the localised increase in the pH due to cathodic reduction of oxygen on different metallic phases of the underlying alloy. Calcite has been previously reported as forming on the surface of corroded silver coins from the wrecks of the *Rapid* (1811) and the *Batavia* (1629), when the surface of the coin is acting as the cathodic site of the corrosion cell [21]. The dominance of aragonite on the edges of the rims of the *Zuytdorp* pewter bottle tops is probably due to localised increases in corrosion rates at the protruding edges, which pick up greater edying of water movement and hence are in a more corrosive microenvironment. It should be remembered that corrosion rates are sensitive to the overall shape and form of an object, with sharp edges being prone to a more rapid rate of deterioration than flat surfaces. Loalised corrosion cells will result in an increased pH and lead to the precipitation of the more kinetically labile aragonite. The presence of only aragonite on the inside of ZT 3359 is a clear indication that with the more restricted water movement on the inside of the pewter bottle caps allowed a more alkaline microenvironment to develop and so precipitate the less stable aragonite.

The dominant species found on the tin alloys on the *Intan* site are associated with aerobic corrosion of both tin and the other alloying elements. For pewter objects, there was a dominance of lead corrosion poducts when the alloy composition was hyper-eutectoid and a dominance of tin corrosion products when the alloy was hypo-eutectoid. For pewters having essentially a eutectoid composition, the tin-rich or lead-rich phases were selectively attacked, and this variation appears to be consistent with changes in the burial microenvironment. The combined x-ray diffraction data and SEM quantitative analysis has provided a sensitive probe into the nature of events on the *Intan* site over the last one thousand years. The presence of anaerobic corrosion products of lead, silver and copper is consistent with the site having been buried for some time before becoming exposed once more [22–24]. It is interesting to note that there was no evidence of anglesite, $PbSO_4$ on the *Intan* site, given its dominance on cooler sites such as the *Rapid* and the *Zuytdorp*. The predominance of cerussite and one sample of hydrocerussite on the *Intan* site is more consistent with corrosion studies on lead in synthetic seawater[25]. This may indicate that other agents, such as microscopic algae absorbed onto the surface of lead objects, may well have a major bearing on the energy associated with crystallisation of specific corrosion products. Given a general knowledge of the range of pH values for marine sediments and the mixture of aerobic and anaerobic corrosion products on the bronze ingot 210-6, it should be possible to develop a range of E_h and pH for the *Intan* wreck which may be of assistance to the maritime archaeologists in developing interpretation of the distribution of materials, and their survival for more than a thousand years, over this rather special wrecksite.

Acknowledgements

We would like to thank Jeffrey Beng and Anna Fletcher of the Materials Institute of Western Australia for assistance in the analyses of the corrosion matrices. The Trustees and Executive Director of the Western Australian Museum are thanked for financial support.

References

1. USSR Ministry of Defence (1974) *Atlas of the Oceans – Pacific Ocean*, USSR Naval Branch, Pergamon Press, Oxford, England
2. Mathers, W. & Flecker, M., (1997) "Archaeological Recovery of the Java Sea Wreck", Pacific Sea Resources, p 65.
3. MacLeod, I.D. & North, N.A. (1982) "Conservation of a composite cannon – *Batavia* (1629)", *International J. Nautical Archaeology* 11(3): 213–219.
4. Scott, D., (1991) in *Metallography and microstructure of ancient and historic metals"*, Getty Conservation Institute, J Paul Getty Museum, USA, p 28.
5. Chase, W.T., (1994) "Chinese Bronzes: Casting, Finishing, Patination and Corrosion" in *Ancient and Historic Metals Conservation and Scientific Research*, ed D.A. Scott, J. Podany, B.B. Considine, (Getty Conservation Institute, 1994): 85–117.
6. MacLeod, I.D. (1983) "Report on the crystals found on metal fragments and on bamboo from the Pattaya wreck site" in "The excavation of the Pattaya wreck site and survey of three other sites in Thailand 1982". J. Green and R. Harper, *Australian Institute Maritime Archaeology Special Pub.* No 1, pp 80–82.
7. Goldberg, E. D., (1957) "Biogeochemistry of trace metals", *Geological Society of America Memoirs* 67, p 345.
8. Degens, E.T., (1965) "Minerals of Low Temperature and Aqueous Formation: Carbonates" in *Geochemistry of Sediments: A Brief Survey*, Englewood Cliff, New Jersey,. pp. 98–141.
9. Cloud, P.E. & Barnes, V.E., (1957) "Early Ordovician Sea in Central Texas", *Geological Society of America Memoirs* 67, 163–214.
10. *Handbook of Chemistry and Physics*, 55th edition, CRC Press, Cleveland, 1974, F198–199.
11. Berndt, M.E., & Seyfried, W.E., Jr., (1999) "Rates of aragonite conversion to calcite in dilute aqueous fluids at 50 to 100°C: Experimental calibration using Ca-isotope attenuation", *Geochimica et Cosmochimica Acta*, 63(3/4), 373–381.
12. Metals Handbook (1973), Volume 8, 8th edition *Mellalographic, structures & Phase Diagrams*, American Society for Metals, Metals Park, Ohio, USA. p 330 & 428–429.
13. MacLeod, I.D. & Wozniak, R. (1996) "Corrosion and Conservation of Lead in Sea Water" *ICOM-Committee for Conservation Preprints 11th Triennial Meeting, Edinburgh, Sept 1996*. James & James, London, p884–890.
14. MacLeod, I.D., (1991) "Identification of corrosion products on non-ferrous metal artefacts recovered from shipwrecks", *Studies in Conservation,* 36, 222–234.
15. MacLeod, I.D. & Wozniak, R., (1997) "Corrosion and conservation of tin and pewter", *Metal 95 – Proceedings of the ICOM -CC Metals Working Group Conference*, Semur-en-Auxois, France 1995, James & James, London, 118–123.
16. Taylor, R.J., & MacLeod, I.D., (1985) "Corrosion of bronzes on shipwrecks: a comparison of corrosion rates deduced from shipwreck material and from electrochemical methods," *Corrosion* 41, 100–104.
17. Campbell H.S. & Mills, D.J. (1977) "A marine treasure trove – metallurgical investigation", *The Metallurgist and Materials Technologists* October, 551–557.
18. Schweizer, F. (1994) "Bronze objects from lake sites: from patina to "Biography" in *Ancient and Historic Metals Conservation and Scientific Research*, Ed D.A. Scott, J. Podany, B.B. Considine Getty Conservation Institute, 33–50.
19. MacLeod, I.D. (1982) "Environmental effects on shipwreck material from analysis of marine concretions", *Archaeometry: an Australasian Perspective (ANU Press)* Ed. W. Ambrose & P. Duerden, 361–367.
20. Refaey, S.A.M., & El Rehim, S.S. Abd., (1996) "Inhibition of chloride pitting corrosion of tin in alkaline and near neutral medium by some inorganic anions", *Electrochimica Acta* 42(4), 667–674.
21. Gali , K., Pavi, M. & Cikovi, N., (1994) "The effect of inhibitors on the corrosion of tin in sodium chloride solution", *Corrosion Science*, 36(5), 785–795.
22. Riley J.P. & Skirrow, G.,(1975) *Chemical Oceanography*, Vol 1 2nd edition, Table 6, p 561–562, Academic Press, New York
23. MacLeod, I.D., (1981) "Shipwrecks and applied electrochemistry", *J. Electroanalytical and Interfacial Electrochemistry,* 118: 291–303.
24. MacLeod, I.D. (1989) "Marine corrosion on historic shipwrecks and its application to modern materials", *Corrosion Australasia.* 14(3), 8–14.
25. Beccaria, A.M., Mor, E.D., Bruno G. & Poggi, G. (1982) "Corrosion of lead in sea water," *British Corrosion Journal*, 17 87–91.